Anisotropy of the resistivity saturation in WO_2

V. F. Gantmakher, G. I. Kulesko, and V. M. Teplinskiĭ

Institute of Solid State Physics, Academy of Sciences of the USSR

(Submitted 17 October 1985)
Zh. Eksp. Teor. Fiz. **90**, 1421–1429 (April 1986)

The anisotropy of the electrical resistivity of WO_2 single crystals is measured at temperatures ranging from liquid-helium temperature to 1300 K. In the high-temperature region, where the mean free path l approaches the interatomic spacing a, the resistivity exhibits a tendency toward saturation along some directions and not along others. The anisotropy of the high-temperature correction due to the smallness of l turns out to be stronger than the anisotropy of the regular part of the resistivity, described by the Boltzmann kinetic equation.

1. INTRODUCTION

According to the Boltzmann equation the resistivity ρ of a degenerate electron gas at temperature T above the Debye temperature Θ should increase linearly with temperature. This implies a linear decrease of the mean free path l with increasing temperature. On the other hand, l cannot decrease indefinitely, since, according to the well-known Ioffe-Regel principle, the mean free path cannot be smaller than the electron de Broglie wavelength:

$$l \gtrsim k_F^{-1}. \qquad (1)$$

At electron densities of the order of one per unit cell, the Fermi wave vector k_F is of the order of the inverse interatomic spacing a^{-1}, so that inequality (1) becomes $l \gtrsim a$.

Inequality (1) implies that the growth of the resistivity with increasing temperature should be bounded. This phenomenon, which has come to be called "resistivity saturation," has been the subject of many studies since the paper of Fisk and Webb,[1] who were the first to link the observed behavior[1] of the temperature dependence of the resistivity of Nb_3Sb and Nb_3Sn with the Ioffe-Regel principle. The considerable amount of experimental material accumulated since that time[2–5] shows that a tendency toward saturation of the resistivity is always present[6] when the mean free path of the carriers approaches limit (1). The question is, just how does the approach of limit (1) affect the value of ρ? First of all, we should recall the various effects that are fundamentally linked with the decrease of l and are therefore most interesting.

Let us turn to the $(T,\hbar/\tau)$ plane, taking the Fermi energy ε_F as the characteristic scale for both axes (Fig. 1). The condition for degeneracy of the electron gas, $T < \varepsilon_F$, and condition (1) together define a square on this plane; this square is divided by the diagonal $T\tau = \hbar$ into two triangles. In the lower triangle, $T\tau > \hbar$, the standard kinetic equation is known to apply. All the complications due to small mean free paths l occur in the upper triangle, $T\tau < \hbar$, where the uncertainty of the electron energies due to scattering is greater than the temperature smearing. Here, in particular, the electron-electron interaction changes because during the interaction time $\hbar/T$ the electrons suffer many collisions with the scatterers which determine the value of τ (impurities or phonons).[7,8] Along the upper boundary of the square, $\hbar/\tau = \varepsilon_F$, not only is the kinetic equation manifestly inapplicable but we have neither an accepted realistic theoretical description nor a sufficiently complete experimental picture.

At high temperatures the Gruneisen curve $\rho(T)$, which describes the electrical resistivity due to phonon scattering in the framework of the kinetic equation, asymptotically approaches the straight line $\rho = m/ne^2\tau = \alpha T$. An estimate neglecting numerical factors shows that for a typical metal with $k_F \approx a^{-1}$ and with a deformation potential $D \approx \varepsilon_F \approx e^2/a$, this straight line is close to the diagonal of the square: $T\tau/\hbar \approx 1$. On account of the numerical coefficients the line can actually lie either below the diagonal (curve 1 in Fig. 1) or above it (curve 2). Curve 1 lies in the upper triangle only at low temperatures. Then l and τ are governed by elastic impurity scattering, with a characteristic frequency of $1/\tau_0$. It is known that under these conditions there is a change in the character of the electron-electron[7,8] and electron-phonon[9,10] scattering. For $T \gtrsim \Theta$ the scattering by phonons is quasielastic and in this sense resembles scattering by impurities. Therefore, the physical ideas underlying Refs. 7–10 evidently apply at high temperatures for curve 2 as well.[8,11,12] Specifically, we mean the change in the probability of the electron-electron scattering due to the fact that one electron diffuses in the field of the other, the appearance of an extremum of the density of states at the Fermi level,[8] and the change in the probability of scattering by long-wavelength phonons[9,11] with wave vector $q \ll l^{-1}$.

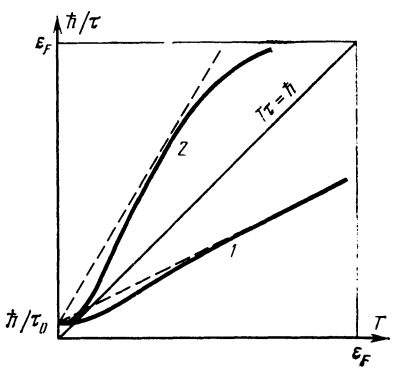

FIG. 1.

 0038-5646/86/040832-06$04.00

The temperature dependence of $\rho(T)$ described by curve 2 is the subject of the present study.

When embarking on an experimental study of this problem, one should bear in mind the following complicating circumstance. Because the experiment is done at high temperatures and because the electronic structure of the investigated metallic systems is complex and, moreover, not always well known, one cannot rule out the possibility that the observed deviations from linearity in $\rho(T)$ are due to specific features of the electron spectrum of the material in question. For example, one can imagine a purely semiconductor effect causing an increase in the number of carriers through excitation of electrons from completely filled bands to the Fermi level. Along curve 2, $\hbar/\tau$ is at first equal to the distance from the completely filled band to the Fermi level, and this should also affect the resistivity.[13] The resistivity should also change when T or $\hbar/\tau$ becomes comparable in order of magnitude with the other characteristic energies describing the electron spectrum (the width of the peak in the density of states at the Fermi level in superconductors with the A-15 structure,[14] the s–d hybridization energy,[15] etc.).

What we have said dictates the strategy of experimental studies of the resistivity saturation. First, one should look for this effect in different classes of materials, and second, one should look for additional variable parameters which would influence the saturation value. In the present study both of these requirements have to a certain degree been met: the resistivity saturation was observed in the transition metal oxide WO_2, which has a metallic conductivity, and a detailed study was made of the anisotropy of the effect.

2. SUMMARY OF DATA ON WO_2

The oxide WO_2 has a monoclinic lattice with the following parameters: $a = 5.5$ Å, $b = 4.9$ Å, $c = 5.7$ Å, $\mathbf{b} \perp \mathbf{a},\mathbf{c}$, $\sphericalangle \mathbf{a},\mathbf{c} = 120.7°$ (see Fig. 2); this is a distorted tetragonal rutile (TiO_2) lattice. As a result of the distortion the period along the fourfold axis c_{rut} is doubled, so that the unit cell contains four WO_2 structural units instead of two. In addition, there is a distortion of the angles, and the only symmetry elements that remain are the twofold axis along **b** and the symmetry plane perpendicular to it (for details see, e.g., Ref. 16).

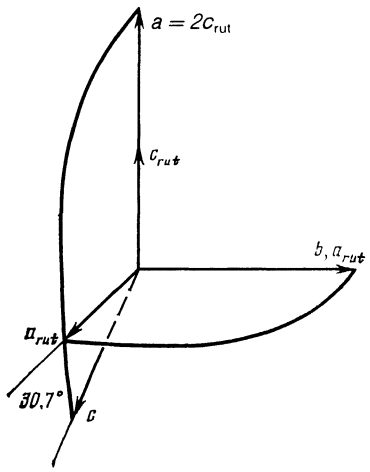

FIG. 2. Location of the crystallographic axes **a**, **b**, and **c** in WO_2 in comparison with the axes $\mathbf{a}_{rut}$ and $\mathbf{c}_{rut}$ in the tetragonal rutile lattice.

Studies using the de Haas–van Alphen effect[16,17] have revealed the presence of two closed sheets of the Fermi surface in WO_2. Both these sheets have a symmetry plane, so that their centers can lie either on the symmetry plane through the Brillouin zone center or on the zone faces parallel to this plane; the number of each of these surfaces per Brillouin zone is not more than two.[17] Both surfaces can be though of as highly distorted ellipsoids protracted along the **a** axis. Their volumes contain approximately $7.2 \cdot 10^{20}$ electrons/cm^3 ($2.4 \cdot 10^{-2}$ electrons per atom) and $1.8 \cdot 10^{20}$ electrons/cm^3 ($0.6 \cdot 10^{-2}$ electron per atom). The effective masses are $0.7m_0$ and $0.5m_0$, respectively, and the Fermi energies are around 2000 K and 3000 K.

Analysis of the different versions with allowance for the fact that WO_2 is a compensated metal shows that the total number of carriers, including those which cannot be revealed with the aid of quantum oscillations, lies in the range $(1.5–3.6) \cdot 10^{21}$ cm^{-3}. If in the formula

$$\rho_a = \hbar k_F / ne^2 a \qquad (2)$$

we set $n = 2 \cdot 10^{21}$ cm^{-3}, $k_F = 0.25$ Å^{-1}, and $a = 5$ Å, we get $\rho_a = 1000$ $\mu\Omega \cdot$ cm. Our measurements (see below) showed that, depending on the direction, the values of the resistivities at room temperature lie between 50 and 180 $\mu\Omega \cdot$ cm. These values are substantially smaller than those known previously [$3 \cdot 10^3$ $\mu\Omega \cdot$ cm (Ref. 2) and $2 \cdot 10^3$ $\mu\Omega \cdot$ cm (Ref. 19)]. The reasons for such large discrepancies with Refs. 18 and 19 are not very well understood. Evidently the structures used in those studes had macroscopic imperfections and contained internal cracks, cavities, etc.

Optical measurements[20] give no reason to doubt the presence of narrow gaps between energy bands: the first peak in the spectrum that can be attributed to interband transitions lies at an energy near $E = 1.75$ eV, and the corresponding absorption edge is approximately equal to 0.9 eV. This allows us to assume that the number of carriers does not change with temperature.

3. EXPERIMENT

The samples started out as WO_2 crystals grown by crystallization from the gas phase[21] and having typical dimensions of 2–4 mm. The crystals were first sorted out by external appearance—the quality of the natural faceting, the absence of cleavage planes or cavities, their dimensions. The orientation of the selected crystals was determined by x-ray diffraction. They were then polished into rods of rectangular cross section. The typical length of the rods was around 3 mm, and the transverse dimensions were from 0.25×0.25 mm to 0.5×0.5 mm. Ordinarily one sample was obtained from each crystal. However, by cutting one of the relatively large crystals with a diamond disk, we were able to prepare from it three samples with different orientations (Nos. 3, 4, and 7). Samples No. 5 and 6 were also obtained from one crystal.

The orientation of the samples, the area of their trans-

TABLE I.

Sample No.	Orientation θ	Orientation φ	Cross sectional area, mm²	ρ_{295}, μΩ·cm	ρ_0, μΩ·cm	ρ_{sat}, μΩ·cm
+ 1	0	–	0.47×0.48	47.4	0.8	∞
+ 2	0	–	0.27×0.24	47.0		∞
+ 3	90	90	0.36×0.35	70.0	0.6	∞
4	90	60	0,37×0.32	78.6	0,9	5600
5	50	40	0.28×0.27	112.7	1.5	2800
6	60	−30	0,32×0.26	144.0	1.9	2600
7	90	−30	0.32×0.31	161.1	1,5	2400
8	90	10	0.54×0.44	168.2	1.7	2400
+ 9	90	0	0.33×0.30	176.5	3,1	2300
+ 10	90	0	0.30×0.25	177.8		2100

Note. The angles θ and φ define the direction of the axis of the sample: θ is the angle to the **b** axis, $0<\theta<90°$; φ is the angle to the **a** axis in the (**a**,**c**) plane, $-90°<\varphi<90°$; $\varphi=-60°$ corresponds to the **c** axis. The crosses indicate samples whose axis was directed along (or nearly along) one of the principal axes of the tensor $\hat{\rho}$.

verse cross section, their room-temperature resistivity ρ_{295}, and their residual resistivity ρ_0 are given in Table I. For convenience we also show the value of ρ_{sat}, the meaning of which is discussed in the following section [see Eq. (5)]. The resistivity ratio ρ_{295}/ρ_0 for all the samples lay between 60 and 120.

The samples were mounted in a special ceramic holder, secured by springs made of W + 5%Re wire (0.2 mm in diameter), which doubled as electrical contacts. The current contacts (the springs) were placed against the ends of the rod, and the potential contacts were placed against one of the lateral surfaces. The ends of the potential leads were sharpened in order to decrease the uncertainty in the point of contact of the lead with the sample. The distance between contacts (usually about 0.7 mm) and the transverse dimensions of the samples were measured on a comparator to an accuracy of 1–2%.

The resistivity tensor at room temperature was determined from the measured value of $\rho_{295}-\rho_0$. Its components and principal axes are

$$\rho^{(1)}=50\ \mu\Omega\cdot\text{cm},\ \rho^{(2)}=70\ \mu\Omega\cdot\text{cm},\ \rho^{(3)}=180\ \mu\Omega\cdot\text{cm}; \quad (3)$$

axis 1 is along **b**, and axes 2 and 3 lie in the (**a**,**c**) plane, with axis 3 forming an angle of about 8° with the **a** axis (see Fig. 3).

The low-temperature measurements were made in a helium cryostat, the high-temperature measurements in a vacuum oven at vacuums down to $5\cdot10^{-8}$ torr. The temperature was measured by means of a thermocouple placed next to the sample.

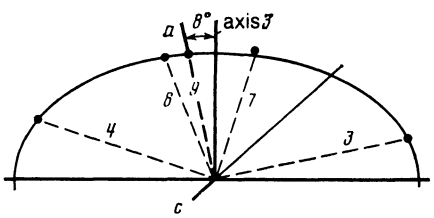

FIG. 3. Cross section of the characteristic surface of the resistivity tensor in the (**a**,**c**) plane. The dashed lines are labeled with the sample number.

4. THE RESULTS AND THEIR PROCESSING

The main result can be stated as follows. The resistivity of WO_2 exhibits a tendency toward saturation in the directions in which ρ is large but not in the directions in which ρ is small. This is demonstrated by Fig. 4, which shows the experimental $\rho(T)$ curves for the samples with the maximum (**J**||**a**) and minimum (**J**||**b**) values of ρ_{295}. The $\rho(T)$ curves for the rest of the samples all lie between these two curves.

For a qualitative interpretation of the results, we made the usual attempt to isolate from the $\rho(T)$ curve the "ideal" part due to processes described by the Boltzmann equation. This was difficult because even for the ideal part an analytical expression exists for arbitrary electron and phonon spectra only in the asymptotic limit,

$$\rho_{id}=\alpha T\ \ (T\gg\Theta), \quad (4)$$

and the analytical form of the high-temperature corrections in which we are interested is really not known at all. Let us first discuss ρ_{id} in somewhat more detail. In a model with a spherical Fermi surface and a Debye phonon spectrum,

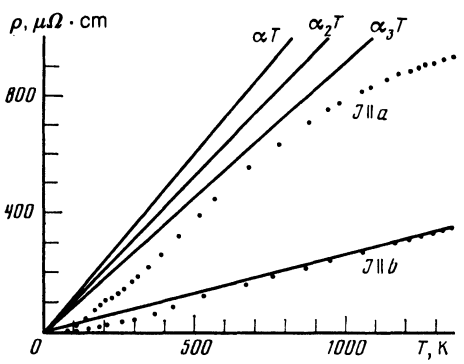

FIG. 4. The $\rho(T)$ curves for two directions of the current. For the meaning of the straight lines with slopes of α, α_2, and α_3, see text [Eqs. (5), (7), and (8)].

$\rho_{id}(T)$ is described by the Grüneisen function. At $T = \Theta$ the value of this function still falls below straight line (4) by 6%, and so asymptotic expression (4) can be used only above $T \gtrsim (1.5\text{–}2)\Theta$. For this particular model, this circumstance is not very important because $\rho_{id}(T)$ is essentially known over the entire temperature interval. The situation is different if allowance is made for the fact that the Fermi surface consists of several separate closed sheets and that the phonon spectrum has optical branches. In both cases there is a characteristic temperature Θ_0 at which the new processes, viz., transitions between sheets or scattering by optical phonons, begin. For $T \gg \Theta, \Theta_0$ asymptotic expression (4) is valid as before, but at low temperatures the curve $\rho_{id}(T)$ cannot be calculated without a detailed knowledge of the spectra. These complications of the $\rho_{id}(T)$ curve are undoubtedly present in WO_2. They are clearly seen, for example, on the $\rho(T)$ curve below room temperature for the sample with J||a (Fig. 4). It is hard to say whether they are due to scattering by optical phonons or to interband transitions—most likely both factors operate. It is clear, however, that one cannot use the Grüneisen curve to describe $\rho_{id}(T)$ in WO_2. In analyzing the curves we have therefore used only the data for $T \gtrsim 700$ K, assuming that by these temperatures $\rho_{id} \propto T$. The residual resistivity ρ_0 of our samples at these temperatures was always less than 1% of the total and could clearly be neglected.

The further processing depends on the form in which we want to get the deviation from ρ_{id}. The analysis is usually done by the "shunting resistance" formula[22]

$$\rho^{-1} = (\alpha T)^{-1} + \rho_{sat}^{-1} \tag{5}$$

(an ingenious model for justifying this formula is found in Ref. 23). Figure 5, which shows a plot of the data for several of the samples in the coordinates $1/\rho$ versus $1/T$, gives an idea of the accuracy to which α and ρ_{sat} are determined. The systematic deviation of the points from straight lines on the right-hand part of the graph corresponds to an increasing deviation of the Grüneisen curve from straight line (4) as the temperature is lowered.

In all our experiments the deviations from the straight line $\rho_{id}(T)$ were relatively small. It is therefore sensible to assume that the correction $\rho - \rho_{id}$ is small and to seek it in

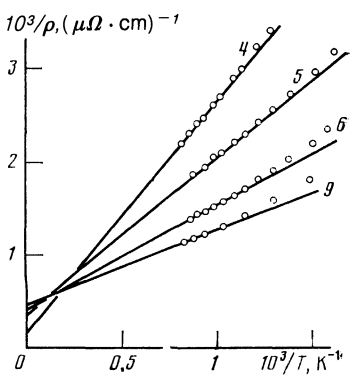

FIG. 5. Temperature dependence of the resistivity for samples No. 4, 5, 6, and 9, plotted in the coordinates $1/\rho$ versus $1/T$.

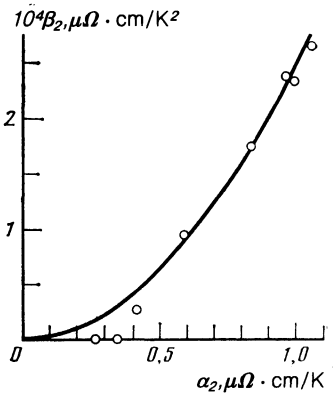

FIG. 6. Result of a processing of the experimental results by the formula $\rho = \alpha_2 T - \beta_2 T^2$.

the form of a power-law function

$$\rho - \rho_{id} = \beta T^r, \quad r > 1. \tag{6}$$

The expansion of expression (5) in a series for $\alpha T \ll \rho_{sat}$ gives $r = 2$:

$$\rho - \rho_{id} = \beta_2 T^2 \tag{7}$$

with a coefficient $\beta_2 = \alpha_2/\rho_{sat}$. In principle, other values of r are also possible. The renormalization of the electron-electron interaction leads to a high-temperature correction proportional to T^3 (Ref. 8):

$$\rho - \rho_{id} = \beta_3 T^3. \tag{8}$$

One can also arrive at a correction of the form (6) with $r = 3$ by analyzing the change in the probability of scattering by long-wavelength phonons (see Sec. 5).

There is, however, one experimental difficulty. The proportionality coefficient α in (4) is unknown *a priori* and must itself be determined from experiment. In Fig. 5, for example, α is determined from the slope of the straight line. However, if (7) or (8) is used instead of (5), the corresponding coefficient (α_2 or α_3) will come out different. The differences in $f2[a]$, α_2, and α_3 for sample No. 9 are illustrated in Fig. 4.

We processed the experimental data by all three formulas. The qualitative result was the same: In going from a sample with a higher resistivity to one with a lower resistivity (i.e., with decreasing α), the correction $\rho - \rho_{id}$ falls off in both absolute and relative value. For example, Fig. 6 shows a plot of $\beta_2(\alpha_2)$, which is the result of a processing by formula (7). The functions $\rho_{sat}^{-1}(\alpha)$ and $\beta_3(\alpha_3)$ have a qualitatively similar appearance.

5. DISCUSSION

In principle, three different versions of the results could be expected in these experiments. First, one might expect that the $\rho(T)$ curve for different directions of the current with respect to the axes of the crystal would change in a self-similar manner on a change of scale along the ρ axis, i.e., that

$$\rho_{sat} \infty \alpha \text{ or } \beta \infty \alpha, \tag{9}$$

where ρ_{sat} and β are given by (5) and (6). This would occur, for example, if the deviation of ρ from ρ_{id} were due to an increase in the number of carriers. Relations (9) also follow from the chain of assumptions $\rho_{sat} \approx \rho_a$, where ρ_a is given by (2), and $\rho_a \propto a$. The first assumption is quite natural. Often it is even assumed[22,6] that Eq. (2) gives ρ_{sat} directly. We have preferred, however, to treat ρ_{sat} as a free parameter. The proportionality $\rho_a \propto \alpha$ is obtained on the assumption that l is isotropic over the Fermi surface. In fact, according to the Boltzmann equation in the τ approximation, we have

$$J = \frac{e^2}{4\pi^3\hbar} \oint \Lambda \frac{Ev_F}{|v_F|} dS_F, \quad \Lambda = \tau v_F \tag{10}$$

(v_F is the Fermi velocity, dS_F is the element of the Fermi surface). If $|\Lambda| = \text{const}$, then all the anisotropy reduces to a purely geometric integral, which enters both (2) and (4). Whatever the case, version (9) is categorically refuted by experiment.

The version $\rho_{sat} = \text{const}$ is also refuted by experiment. If this were the case, then all the straight lines in Fig. 5 would intersect at a common point on the ordinate.

According to our results, a third version—the "enhanced anisotropy" version—obtains in WO_2. The anisotropy of correction (6) is greater than the anisotropy of ρ_{id}. This statement requires some explanation. In expansion (6) the quantities $\hat{\rho}_{id} = \hat{\alpha}T$ and $\hat{\beta}$ are tensors. Because of the low symmetry of the WO_2 crystal, only one of the principal axes has a fixed direction—along the **b** axis. It follows from Fig. 6, however, that the other two axes either coincide or nearly coincide, so that β is a monotonic function of α. It would be natural to compare the ratios of the diagonal components of the tensors $\hat{\alpha}$ and $\hat{\beta}$ written in the principal axes and to seek the exponent s in the expression

$$\beta^{(i)}/\beta^{(k)} = (\alpha^{(i)}/\alpha^{(k)})^s \quad (i, k = 1, 2, 3). \tag{11}$$

However, we were actually able to measure only $\beta^{(3)}$ [cf. the notation in (3)], while for the other two components it turned out that $\beta^{(1)} \approx \beta^{(2)} \approx 0$, and for them we could only estimate an upper limit. The estimate shows that

$$s \gtrsim 2. \tag{12}$$

It should be clarified that, since the sign of the high-temperature correction is negative, the "enhanced anisotropy" of the correction means that the anisotropy of ρ decreases with increasing T.

To demonstrate the importance of this kind of experimental observation, we show that an "enhanced anisotropy" with $r = 3$ is obtained for the correction to the resistivity due to the decrease in the scattering by long-wavelength phonons. Suppose that the resistivity is governed by electronic transitions between different sheets of the Fermi surface, so that the transport cross section is approximately equal to the total scattering cross section. Then for $T \gg \Theta$ the standard procedure of starting from the kinetic equation leads to the expression

$$\rho \propto T \int_0^{q_{max}} q\, dq, \tag{13}$$

where q_{max} is the maximum momentum of the phonons scattering the electrons:

$$q_{max} \approx k_F. \tag{14}$$

According to Ref. 24, the probability of scattering by a phonon of momentum q for $ql \ll 1$ is smaller by a factor of ql than in the case $ql \gg 1$, for which (13) holds. Therefore, for sufficiently small l we can break the integral in (13) into two:

$$\int_0^{k_F} q\, dq \to l \int_0^{1/l} q^2\, dq + \int_{1/l}^{k_F} q\, dq, \quad 1/l < k_F. \tag{15}$$

Hence

$$\rho = \rho_{id}[1 - {}^1/_3 (k_F l)^{-2}] = \rho_{id}[1 - c(\rho_{id}/\rho_a)^2] \tag{16}$$

[the coefficient 1/3, of course, does not make much sense, if for no other reason than because relation (14) is extremely approximate; we have therefore replaced it by the symbol c]. After substituting (4), we obtain the correction in form (8) with a coefficient $\beta_3 \propto \alpha_3^3$. This implies that the correction to the resistivity has an "enhanced anisotropy" of the kind observed in experiment. However, it seems premature to conclude that the tendency toward saturation of the resistivity in WO_2 is due to a decrease in the phonon scattering efficiency.

We remark in closing that, as we see from Fig. 4, from a formal point of view the resistivity of WO_2 decreases with increasing temperature. Something similar is also observed in other materials. Of particular interest in this regard are the data for elemental metals.[25] For large absolute values of the resistivity, yttrium[26] and the metals of the titanium group (titanium,[27] zirconium, hafnium[25]) have been found to exhibit at high temperatures a tendency toward saturation accompanied by a decrease in the anisotropy. This gives us reason to assume that the behavioral regularities observed in WO_2 are quite general.

We are grateful to L. A. Klinkova for furnishing the WO_2 crystals, to N. P. Ushakovskaya for the x-ray orientation of the crystals, and to D. E. Khmel'nitskiĭ for helpful discussions.

[1] Z. Fisk and G. W. Webb, Phys. Rev. Lett. **36**, 1084 (1976).
[2] C. S. Sunandana, J. Phys. C **12**, L165 (1979).
[3] A. C. Lawson, Phys. Lett. A **107**, 45 (1985).
[4] K. Mori, N. Tamura, and Y. Saito, J. Phys. Soc. Jpn. **50**, 1275 (1981).
[5] P. Nedellec, F. V. Creppy, L. Dumoulin, and J. P. Burger, Phys. Lett. A **111**, 67 (1985).
[6] M. Gurvitch, Phys. Rev. B **28**, 544 (1983).
[7] A. Schmid, Z. Phys. **271**, 251 (1974).
[8] B. L. Al'tshuler and A. G. Aronov, Zh. Eksp. Teor. Fiz. **77**, 2028 (1979) [Sov. Phys. JETP **50**, 968 (1979)].
[9] A. Schmid, Z. Phys. **259**, 421 (1973).
[10] B. L. Al'tshuler, Zh. Eksp. Teor. Fiz. **75**, 1330 (1978) [Sov. Phys. JETP **48**, 670 (1978)].
[11] N. Morton, B. W. James, and G. H. Wostenholm, Cryogenics **18**, 131 (1978).
[12] R. B. Laughlin, Phys. Rev. B **26**, 3479 (1982).
[13] B. Chakroborty and P. B. Allen, Phys. Rev. Lett. **42**, 736 (1979).
[14] R. W. Cohen, G. D. Cody, and J. J. Halloran, Phys. Rev. Lett. **19**, 840 (1967).
[15] M. Weger, R. A. deGroot, F. M. Mueller, and M. Kaveh, J. Phys. F **14**, L207 (1984).

[16]E. P. Vol'skiĭ and V. M. Teplinskiĭ, Zh. Eksp. Teor. Fiz. **63**, 1048 (1972) [Sov. Phys. JETP **36**, 550 (1973)].
[17]E. P. Vol'skiĭ and V. M. Teplinskiĭ, Zh. Eksp. Teor. Fiz. **69**, 733 (1975) [Sov. Phys. JETP **42**, 373 (1975)].
[18]D. B. Rogers, R. D. Shannon, A. W. Sleight, and J. L. Gillson, Inorg. Chem. **8**, 841 (1969).
[19]L. Ben-Dor and Y. Shimony, Mat. Res. Bull. **9**, 837 (1974).
[20]M. A. K. L. Dissanayake and L. L. Chase, Phys. Rev. B **18**, 6872 (1978).
[21]A. V. Babushkin, L. A. Klinkova, and E. D. Skrebkova, Izv. Akad. Nauk SSSR Neorg. Mater. **13**, 2114 (1977).
[22]H. Wiesmann, M. Gurvitch, H. Lutz, A. Ghosh, B. Schwarz, M. Strongin, P. B. Allen, and J. W. Halley, Phys. Rev. Lett. **38**, 782 (1977).
[23]M. Gurvitch, Phys. Rev. B **24**, 7404 (1981).
[24]A. B. Pippard, Philos. Mag. **46**, 1104 (1955).
[25]V. E. Zinov'ev, Kineticheskie Svoistva Metallov pri Vysokikh Temperaturakh (Spravochnik) [Kinetic Properties of Metals at High Temperatures (Handbook)], Metallurgiya, Moscow (1984).
[26]V. E. Zinov'ev, A. L. Sokolov, P. V. Gel'd, G. E. Chuprikov, and K. I. Epifanova, Fiz. Tverd. Tela (Leningrad) **17**, 3617 (1975) [Sov. Phys. Solid State **17**, 2353 (1975)].
[27]V. E. Zinov'ev, Fiz. Tverd. Tela (Leningrad) **20**, 2249 (1978) [Sov. Phys. Solid State **20**, 1298 (1978)].

Translated by Steve Torstveit